npj | materials degradation

Article

Published in partnership with CSCP and USTB

https://doi.org/10.1038/s41529-025-00706-3

Rapid screening of the stability of polyacrylamide-based hydrogel coatings via droplet microarray analysis and interpretable machine learning

Jingzhi Yang[1], Yami Ran[1], Yuting Jin[2], Annan Kong[1], Mingyue Zhang[1], Lingwei Ma[1,2,3] ✉ & Dawei Zhang[1,2,3] ✉

The unsatisfactory stability of hydrogel coatings hinders their functional and service performance. Until now, the development of high-performance hydrogel coatings largely relies on the intuition and prior experience of researchers. Machine learning, as a powerful engine for material design, was demonstrated to accelerate the development of hydrogels with desired properties. However, the scarcity of labeled data of the target property is a fundamental challenge. Herein, we develop a miniaturized high-throughput evaluation method of hydrogel coatings. This method achieved a rapid and parallel investigation of the stability of a large number of unique acrylamide-based hydrogel coatings. Moreover, a list of main feature descriptors was screened and their quantitative contributions to coating stability were analyzed via interpretable machine learning technology. A new ternary hydrogel coating was prepared to validate the accuracy of the machine learning strategy. This advanced methodology facilitated the rational design of high-performance hydrogel coatings.

Hydrogels are sample spanning polymer networks swelled with water that have the potential to mimic the mechanical properties and biological functions of natural tissues[1]. Hydrogels exhibit a diverse array of chemical compositions and network topologies, endowing them with high customizability. Functional hydrogels are appealing candidates for use as stimuli-responsive[2], drug delivery[3], lubricating[4], and antifouling[5], systems. Integrating hydrogels as surface coatings on various substrates is promising to impart above functionalities of substrate materials while retaining their inherent advantages[6]. Benefiting from these particular features, hydrogel coatings play an essential role in the field of implanted medical devices, biosensors and anti-marine creature fouling[7].

However, hydrogels generally exhibit undesirable stability when coated on the substrate. Due to the hydrophilic properties, hydrogels swell easily in aqueous solution. This swelling behavior of hydrogels is often inconsistent with that of the substrate material, leading to its partial or complete detachment. The swellability of hydrogels can be tuned by incorporating hydrophobic monomers[8] or nanosheets[9]. Meanwhile, the weak mechanical properties of hydrogel make it unstable on the substrate surface. Researchers usually introduced the hydrophilic-hydrophobic interactions[10] or hydrogen bonds into the polymer network[11] to overcome this problem. The integrity and functionality of the hydrogels may further be impaired by harsh environments such as strong bases and acids, which could break the crosslinks in the hydrogel network[12]. Similarly, researchers enhanced the hydrogel coating stability under acids (pH ~ 1), bases (pH ~ 14) and salt solutions (1 M NaCl) by incorporating hydrophobic groups and MXenes[13]. The existing studies indicated that swelling behavior, mechanical properties and network degradation all have an impact on the stability of hydrogel coatings. The challenges faced in the design of hydrogel coatings with high stability are extremely complex. At present, the development of hydrogel coatings mainly relies on the intuition and experience of scientists. In the harsh environment where the degradation and failure mechanism of hydrogel coatings remains unclear, this trial-and-error methodology gradually became inefficient[14].

Recently, machine learning has been increasingly applied to accelerate material design and development. This intelligent technology could "learn" from the data on its own to predict properties of unknown material and reveal the rules underlying the datasets[15–17]. Researchers optimized the mechanical and electrical properties of acrylamide (AM)/alginate double-

[1]National Materials Corrosion and Protection Data Center, Institute for Advanced Materials and Technology, University of Science and Technology Beijing, Beijing, China. [2]Institute of Materials Intelligent Technology, Liaoning Academy of Materials, Shenyang, China. [3]School of Advanced Materials Innovation, University of Science and Technology Beijing, Beijing, China. ✉e-mail: mlw1215@ustb.edu.cn; dzhang@ustb.edu.cn

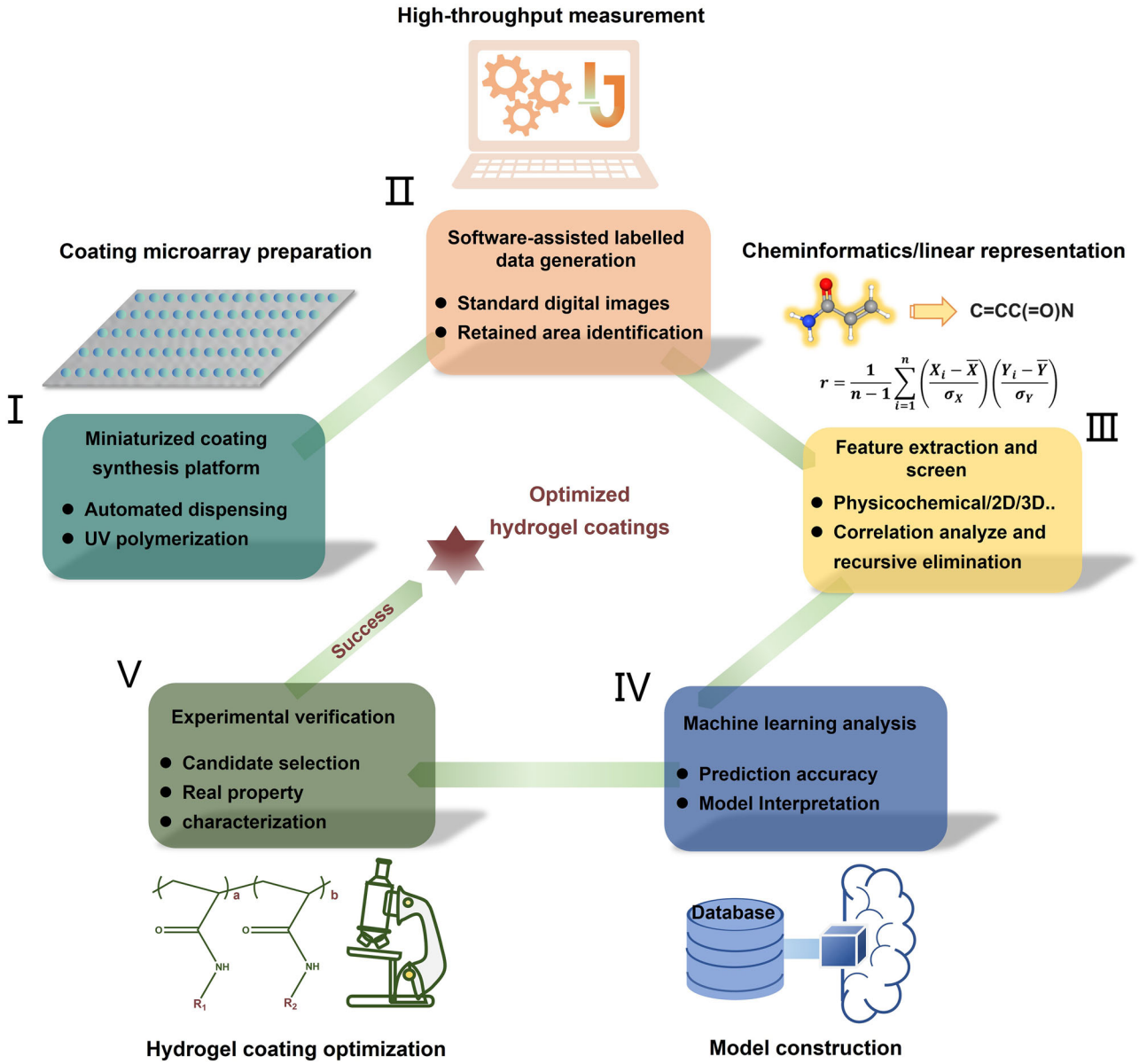

Fig. 1 | Workflow of droplet microarray platform and machine learning integrating strategy for the investigation of polyacrylamide-based hydrogel coatings.

network hydrogels by regulating the concentrations of each component via machine learning technology. Meanwhile, machine learning results revealed that the concentrations of AM monomer, ammonium persulfate, and *N,N'*-methylene diacrylamide significantly influence the hydrogel performance[17]. Nonetheless, as a data-driven approach, ML-assisted materials design is often limited by the availability of quality data, which is traditionally obtained by laborious one-by-one synthesis and characterization experiments. The development of a robotic experimental platform enables automated and high-throughput materials synthesis and characterization[18,19]. This experimental manner could substantially accelerate the generation of high-quality data[20]. The closed loop approaches that couple automated experiments to ML technology have been successfully demonstrated in some fields, including catalysts[21], photovoltaics[22], and battery materials[23], and also hold great promise to promote the investigation of the hydrogel coatings.

In this work, we developed an effective method that integrates machine learning technology and a high-throughput experimental approach based on droplet microarray printing to investigate and design the polyacrylamide-based hydrogel coatings with high stability under harsh conditions. This droplet microarray platform could achieve a miniaturized and parallel batch synthesis of hydrogels. Particularly, a library of 117 hydrogel-based coatings assembled from 9 acrylamide-based monomers was rapidly created using this platform. To elucidate the underlying relationship between coating formulation and the observed performance, a set of main molecule feature descriptors was identified based on correlational analysis and recursive feature elimination. Post hoc analysis of our model provided the rules into how hydrogel may remain stable as surface coatings. Following this rule, some new hydrogel coatings were prepared and verified experimentally. This method demonstrated an efficient avenue for accelerated design of high-performance hydrogel coatings.

Results

Screening strategy

Figure 1 summarizes the workflow for the stability investigation of polyacrylamide-based hydrogel coating via droplet microarray platform and machine learning integrating strategy. The workflow primarily consists of five parts: (i) Miniaturized parallel hydrogel coating synthesis enabled by molecule solution dispensing technology; (ii) ImageJ software assisted rapid

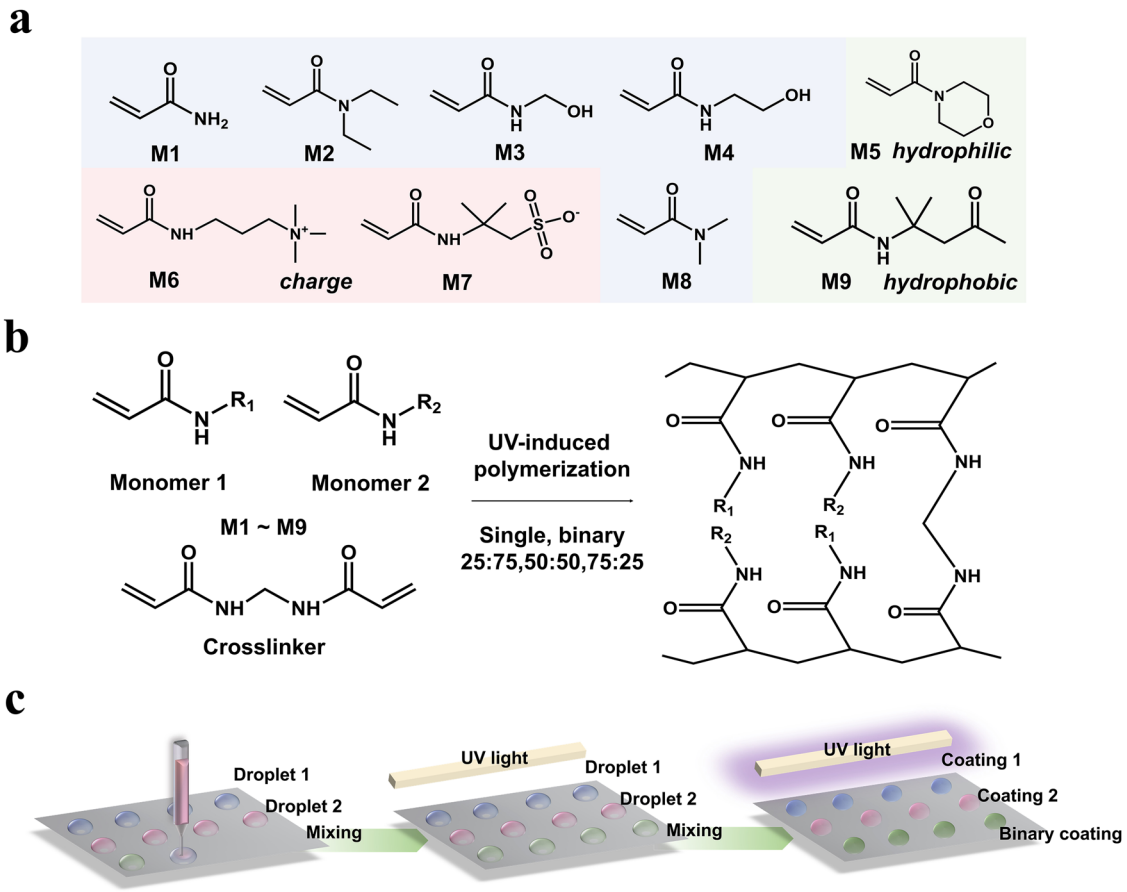

Fig. 2 | The monomer selection and preparation method of polyacrylamide-based hydrogel coating microarrays. a Monomers for combinatorial synthesis via photopolymerization: acrylamide (M1), diethylacrylamide (M2), hydroxymethylacrylamide (M3), hydroxyethylacrylamide (M4), acryloylmorpholine (M5), (acrylamidopropyl)trimethyl-ammonium (M6), 2-acrylamido-2-methylpropane sulfonic acid (M7), dimethylacrylamide (M8), N-isopropylacrylamide (M9). **b** The polymerization method used for hydrogel preparation. **c** Schematic diagram of the process to prepare a hydrogel coating microarray.

evaluation of the hydrogel coating stability under harsh conditions; (iii) Screening of extracted molecular feature descriptors via correlation analyze and recursive elimination; (iv) Machine learning model construction while interpreting using game-theory based SHAP methodology; (v) Selection and synthesis of high-performance coating formulation based on model predication. This droplet microarray high-throughput preparation platform was equipped with a piezoelectric pipetting tip to achieve a precise dispensing of droplets. Benefiting from the high-throughput experimental platform, we developed an efficient and economical method to produce hundreds of hydrogel coatings on one substrate. This method was demonstrated to be generally applicable to prepare and characterize a broad range of hydrogel coatings, such as zwitterion, poly (ethylene glycol) (PEG), 2-hydroxyethyl methacrylate (HEMA)[18,24,25] and polyacrylamide (this work). Moreover, manually analyzing the large amounts of data obtained in high-throughput experiments may be time-consuming and laborious, and it is easy to ignore some underlying information. An interpretable machine learning method could aid us in understanding the molecular features that determined the performance of all of hydrogel coatings we tested. We analyzed the 19 feature descriptors of each coating and elucidated their contribution to stability tendencies. This closed-loop integrating strategy that involved data generation, data analysis and experimental verification had accelerated the investigation of the polyacrylamide-based hydrogel coatings.

Hydrogel coating preparation based on droplet microarray platform

Due to their biocompatibility, polyacrylamide-based hydrogels have extensive applications in biomedical settings[26], such as contact lenses[27], drug delivery systems[28], and anti-biofouling coatings[29]. The stability of polyacrylamide-based hydrogel coatings under physiological conditions is crucial for their longer-term application. To maximize the investigation scope of the stability of polyacrylamide-based hydrogel coatings, 9 commercially available acrylamide-derived monomers were selected, and the molecular structural formula of these monomers were shown in Fig. 2a. They provided wide chemical diversity, including various alkane chain lengths, distinct functional groups, both linear and cyclic aliphatic structures, varying charge properties, and diverse wettability. Relying on the reactivity of the C = C bond and crosslinker Bis, acrylamide-derived monomers can form hydrogel networks through one-step UV-induced free radical polymerization (Fig. 2b). As shown in Fig. 2c, the combinatorial preparation of the hydrogel coatings was achieved via a miniaturized high-throughput manner. According to the preset program, different precursor solutions are sequentially pipetted onto the metal surface and undergo in-situ polymerization to form hydrogel coatings (details were presented in 'Methods'). A library of 117 copolymer hydrogel coatings comprising unique single or binary combinatorial mixtures (75:25, 50:50, 25:75 in mass ratio) was fabricated using these monomers.

The pipetting process was monitored, and the corresponding digital image is shown in Fig. 3a. The top view and side view of the coating microarray images demonstrated the successful preparation and regular distribution of hydrogel coating spots (Fig. 3b, c). A single microarray could consist of 400 (20 × 20) unique coating formulations, and these coatings exhibited the same size and thickness. The optical microscopy image showed that the diameter of each coating spot is approximately 2 mm (Fig. 3d). Moreover, the green and red fluorescent dyes were observed to be

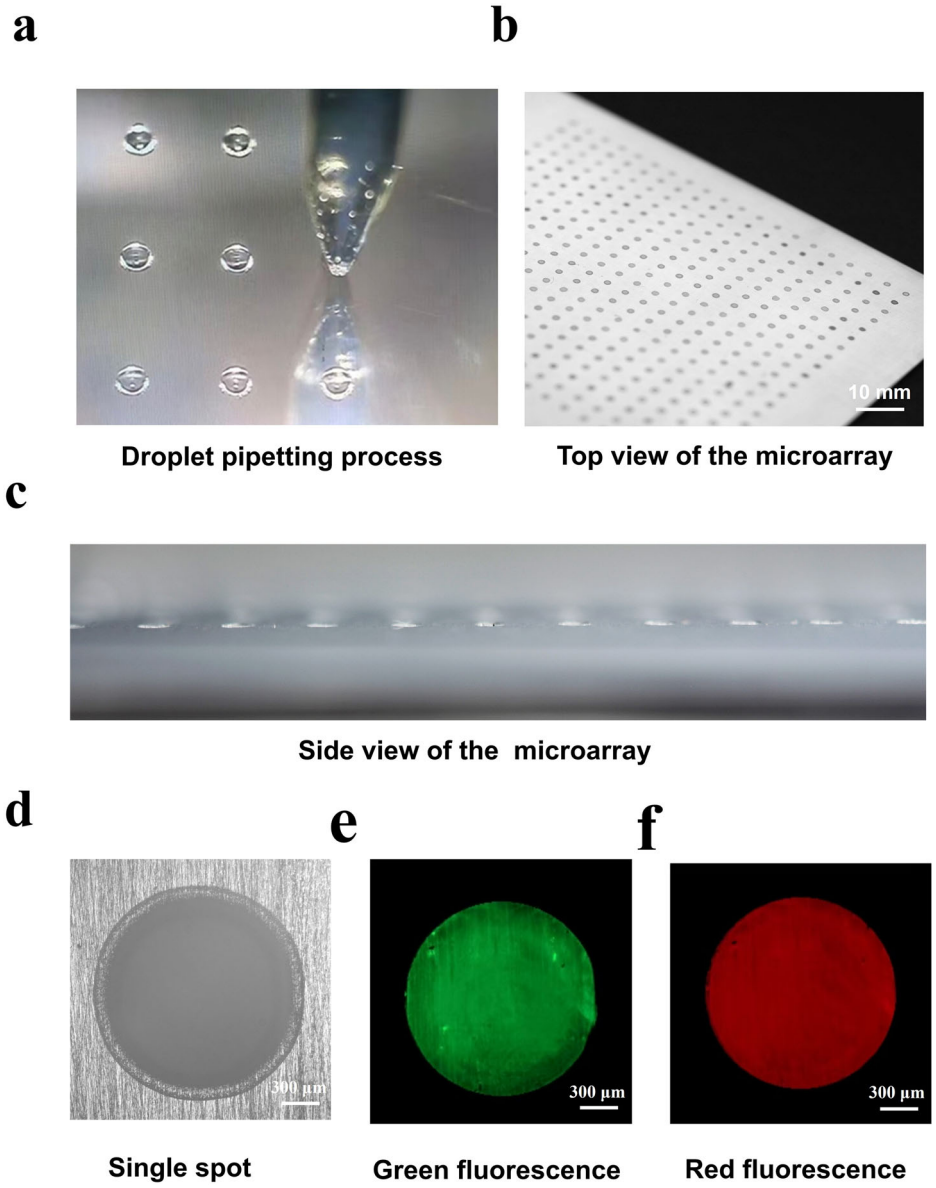

Fig. 3 | The digital and optical microscope images of the microarray. a Droplet pipetting process. **b** Top view of the microarray with a 400 (20 × 20) hydrogel spots. **c** Side view of the microarray. **d** The optical microscopy image of a single spot. **e** Green and **f** red fluorescence images of a single spot.

evenly distributed in the whole spot after preparation of the coating microarray (Fig. 3e, f). This phenomenon confirmed the adequate mixing and homogeneous distribution of the monomers in the hydrogel coating microarrays. The uniform mixing is mainly due to significant turbulence during the drop pipetting[18,25]. The miniaturized high-throughput synthesis paradigm enabled rapid screening of hydrogel coatings.

High-throughput stability evaluation of the hydrogel coating microarrays

From the literature, the monomer and crosslinking would impact the properties of the hydrogel coatings[30–32]. Taking these two parameters as variables, we first examined the water immersion stability of polyacrylamide-based hydrogel coatings. The hydrogel coating spots after the immersion for 48 h were simply classified into intact spots, slightly damaged spots and seriously damaged spots. The typical images of these three types of coatings were shown in Fig. S1, while the damage degree was used to evaluate the immersion stability of coating spots. As shown in Fig. S2, insufficient crosslinker content weakens the elastic properties of the polymer network, leading to poor stability of the hydrogel coating in an immersion environment. On the other hand, excessive crosslinkers leave the hydrogel coatings too fragile to remain stable against swelling[33]. A similar trend was observed when varying the monomer content. Almost all hydrogel coatings at a monomer content of 20 wt.% and crosslinker content of 10 wt.% were demonstrated to remain intact in the water immersion environment (Fig. S2f). Therefore, the above two parameters were fixed at 20% and 10% in subsequent experiments to avoid the coating being damaged by swelling.

Further, a library of hydrogel coatings was built to investigate the impact of different monomer combinations on their stability in the presence of strong base, acid and mixed enzymes. To rapidly evaluate the extent of damage on these hydrogel coatings in a parallel fashion, we used a high-throughput image analysis method to quantitatively measure the retained area of coating spots after immersion in these harsh conditions, respectively. The quantitative measurement process of 10 typical coating spots was shown in Fig. S3. Figure 4a summarized the stability values (hereafter referred to as S_{tab} value) of all hydrogel coatings involving single and binary combinations of M1 to M9. In this 9 × 45 matrix, red and blue squares represented the relatively high and low S_{tab} value, respectively. The hydrogel coatings with optimal S_{tab} value were marked in bright red. Although we were not able to discern clear trends in the stability of the polyacrylamide hydrogel coatings under harsh conditions in their composition, the introduction of hydrophobic monomer M9 generally yielded more hydrogel

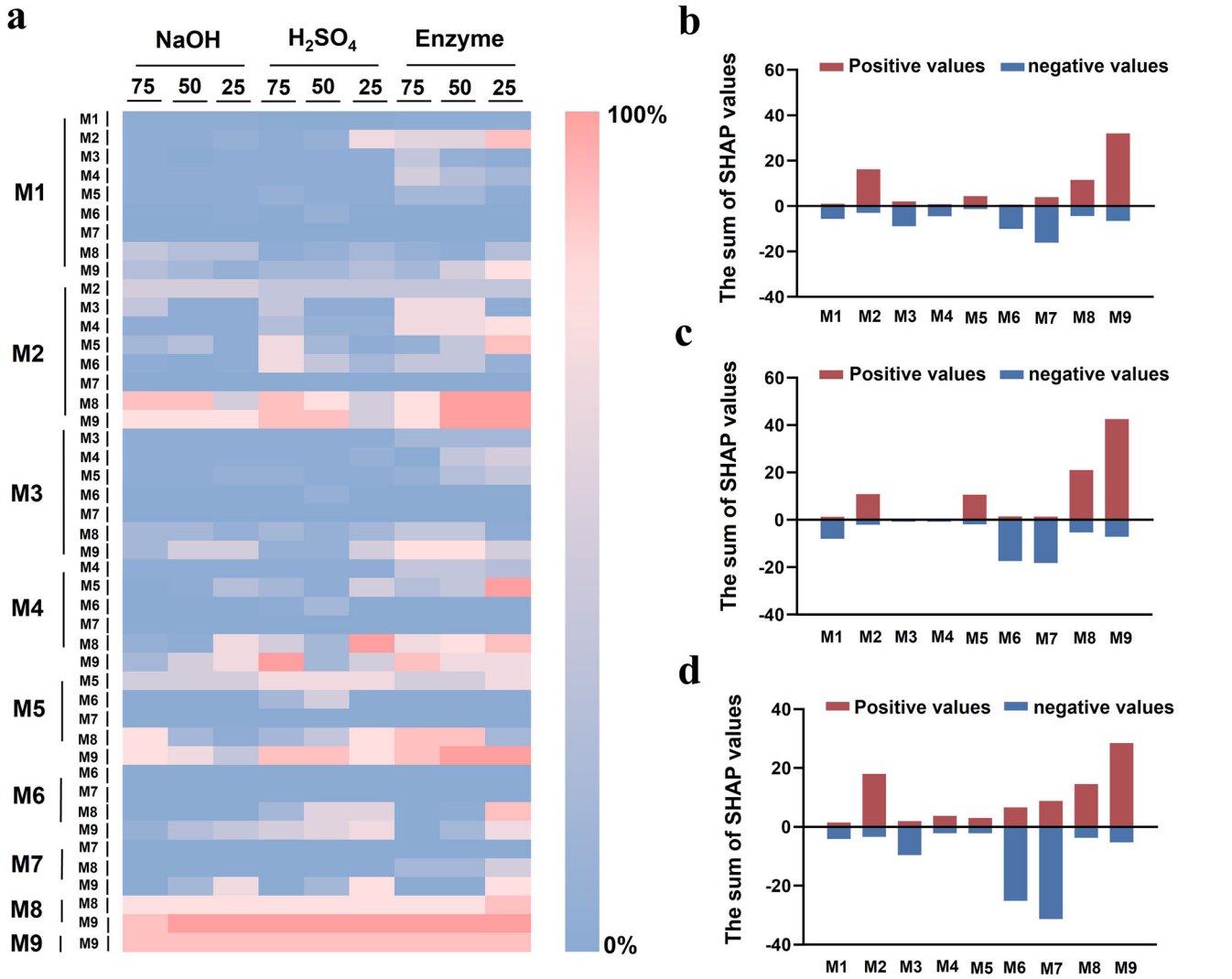

Fig. 4 | The evaluation results of the stability of polyacrylamide-based hydrogel coatings. a Heat map of the S_{tab} value of the single and binary combination of hydrogel coatings using high-throughput assays. The heat map reported the specific compositions of coatings. The vertical axis (on the left) represented the molecular combinations, and the numbers on the horizontal axis (at the top) indicated the proportion of the first monomer (expressed by larger characters). The sum of the proportions of the two monomers was 100. The sum of SHAP values of each monomer for the S_{tab} value of hydrogel coatings after the immersion of **b** strong base, **c** acid and **d** mixed enzyme solution.

coatings with high S_{tab} value. In contrast, a binary combination of M8 and M9 yielded the optimal hydrogel coating that exhibited stability in strong base, strong acid and mixed enzyme solution. Some other formulations such as a 75:25 combination of M4 and M9 or a 50:50 combination of M2 and M8 exhibited excellent stability in the immersion of strong acid and mixed enzyme solution, respectively. The homopolymer prepared by single M8 and M9 monomers exhibited decent stability, but their S_{tab} value was lower compared to the optimal hydrogel coating in the binary combination.

To comprehensively analyze the impact of hydrogel composition on its stability. A machine learning regression model (GBR) was built to fit the relationship between the hydrogel formulation and their S_{tab} value. The GBR model offers robustness to high-dimensional and sparse features, and excels in capturing complex nonlinear relationships[34]. SHAP analysis was used to interpret the machine learning model output. A simple dataset was generated to capture the hydrogel coating formulations, whereby each coating was represented using one-hot encoding based on the mass ratios of the monomers. Subsequently, SHAP analysis was used to interpret the machine learning model output. As shown in Fig. 4b–d, the sum of positive (red color) and negative (blue color) SHAP values for each monomer in all hydrogel coating formulations was displayed separately. The contributions of the monomers to hydrogel coating stability generally exhibited consistent trends in different environments. The results pointed to M2, M5, M8 and M9 facilitating the coatings to be stable under harsh conditions, while the introduction of M1, M3, M6 and M7 was associated with the coating destabilization. Based on the results of SHAP analysis, it can be preliminarily deduced that the linear and charged monomers appear to be harmful for the stability of hydrogel coatings, and monomers with side chains seem to improve the coating stability. This may be attributed to the presence of side chains increases the steric hindrance of the polymer network, enhancing the entanglement between molecular chains[35]. Moreover, the electrostatic repulsion in charged monomers would increase the distance between polymer chains in hydrogels, resulting in a decrease in the tightness of the coating network, thereby impacting the integrity of the hydrogel coatings and reducing their stability[36,37]. Although one-hot encoding of hydrogel coating formulations has revealed some trends in their behaviors, its lack of generalization ability restricts its application in guiding the design of hydrogel coatings in unexplored chemical spaces.

Identifying main molecular feature descriptors for the coating stability

To help us in identifying the main molecular features giving rise to the stability of polyacrylamide-based hydrogel coatings under different

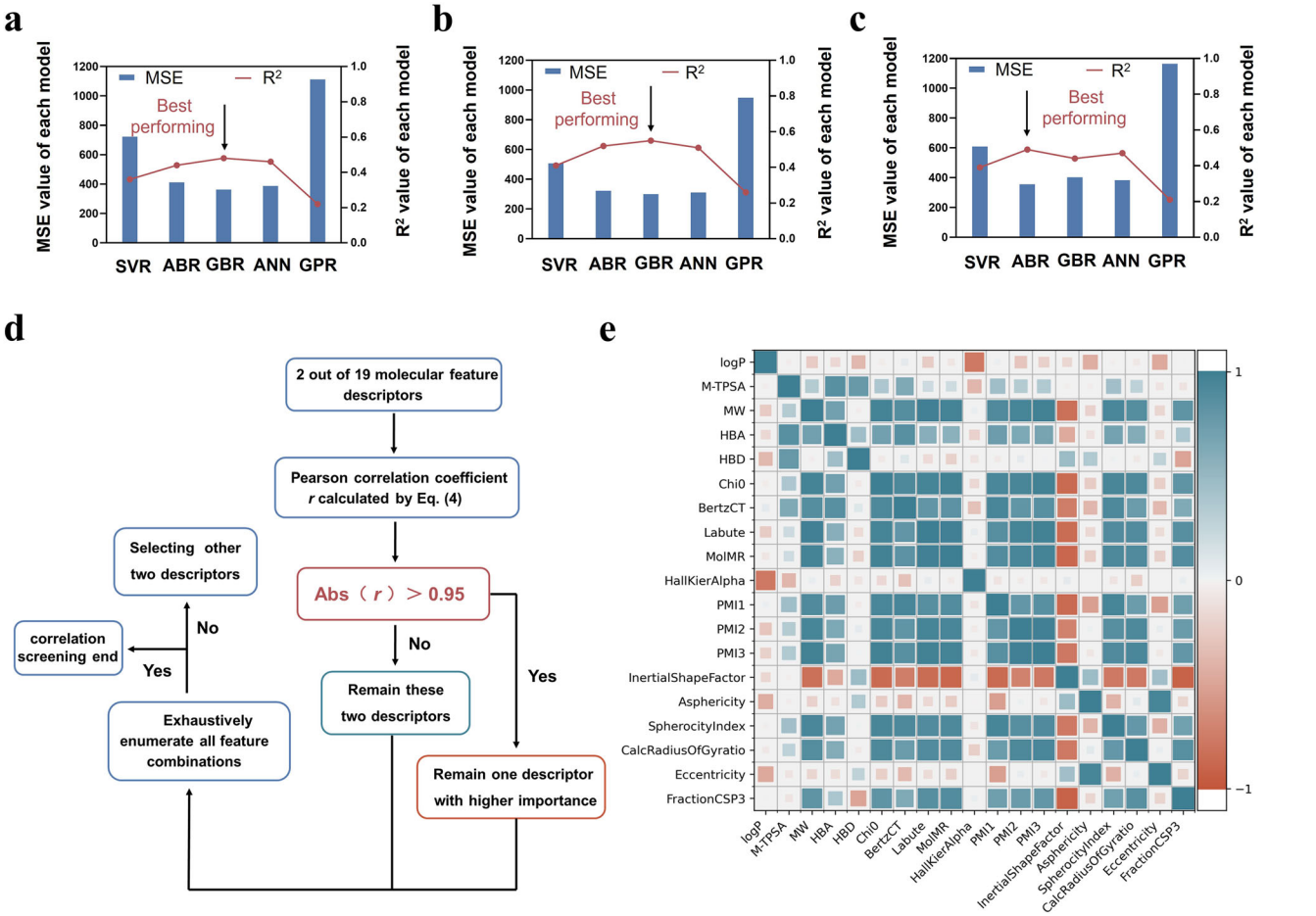

Fig. 5 | The machine learning model evaluation and correlation analysis results. Prediction accuracy (lower MSE value and higher R^2 value represent higher accuracy) of SVR, ABR, GBR, ANN and GPR regression models for the S_{tab} value of hydrogel coatings in **a** strong base, **b** strong acid and **c** mixed enzyme environments. **d** The flow chart showed the correlation screening process. **e** Pearson correlation coefficients between all molecular feature descriptors, where cyan and brown represented positive and negative correlations, respectively, and deeper colors indicated stronger correlations.

conditions, we first extracted a total of 19 types of feature descriptors for each monomer. These descriptors were classified into four categories, including physicochemical descriptors, 2D molecular graph descriptors, 3D shape descriptors and hydrogen-bonding descriptors. Each polyacrylamide molecule was first represented as a simplified molecular input line entry system (SMILES) string, and subsequently their feature descriptor extraction could be implemented in the RDKit library[38]. The brief introduction of these 19 feature descriptors was summarized in Table S1. The feature descriptors for the hydrogel coating were obtained by calculating the weighted average of monomer descriptor values according to the specific coating composition[26]. We built five different regression models and used these 19 feature descriptors as the input. The MSE and R^2 values were used to evaluate the prediction accuracy of the regression models, and the model with the minimal MSE and maximal R^2 value was selected for further study. As shown in Fig. 5a–c, among these regression models, the best model corresponding to predicting the S_{tab} value of hydrogel coatings in strong base, strong acid and mixed enzyme conditions was the GBR, GBR and ABR, respectively. The MSE values of the models ranged from 300 to 400. Based on the best models, we performed the feature screening on these 19 molecular feature descriptors using correlation analysis and recursive elimination.

Figure 5d, e showed the correlation screening process and the correlation coefficient r value between 19 molecular feature descriptors. For any pair of feature descriptors exhibiting a strong correlation, two machine learning models were built using one descriptor from the pair along with the remaining descriptors as inputs. After evaluating the prediction accuracies of the two models, the feature descriptor corresponding to the less accurate model was excluded from the input dataset. In the machine learning model to predict the S_{tab} value of hydrogel coatings in strong base, strong acid and mixed enzyme solutions, the same 12 feature descriptors were obtained after a correlation screening process. As shown in Fig. 6a–c, the prediction accuracy of the model increased after correlation screening (evidenced by the decreased MSE value). The redundant information in the input dataset led to overfitting or noise amplification of the model[39].

These 12 feature descriptors were further screened using recursive elimination. With the recursive elimination process proceeding, the prediction accuracy of the model gradually increased. Eliminating feature descriptors that weakly correlated with the hydrogel coating stability further improved the prediction performance of the models[40]. Notably, the prediction accuracy of the three models changed from an upward trend to a downward trend when the number of features was reduced to 5, 5, and 6, respectively. It indicated that the weakly correlated descriptors have all been screened out, and the recursive elimination could be terminated at this point. Finally, 5, 5, and 6 feature descriptors were identified as the main descriptors for predicting the S_{tab} value of hydrogel coatings under strong base, strong acid, and mixed enzyme environments, respectively. The detailed main feature identifying process using correlation analysis and recursive elimination was visualized in Fig. 6d–f. The remaining feature descriptors after each round of recursive elimination can be clearly observed (marked with a blue rhombus). Red rhombuses highlighted the main feature descriptors obtained after the whole screening process, which were considered the most determinant set of descriptors for hydrogel coating

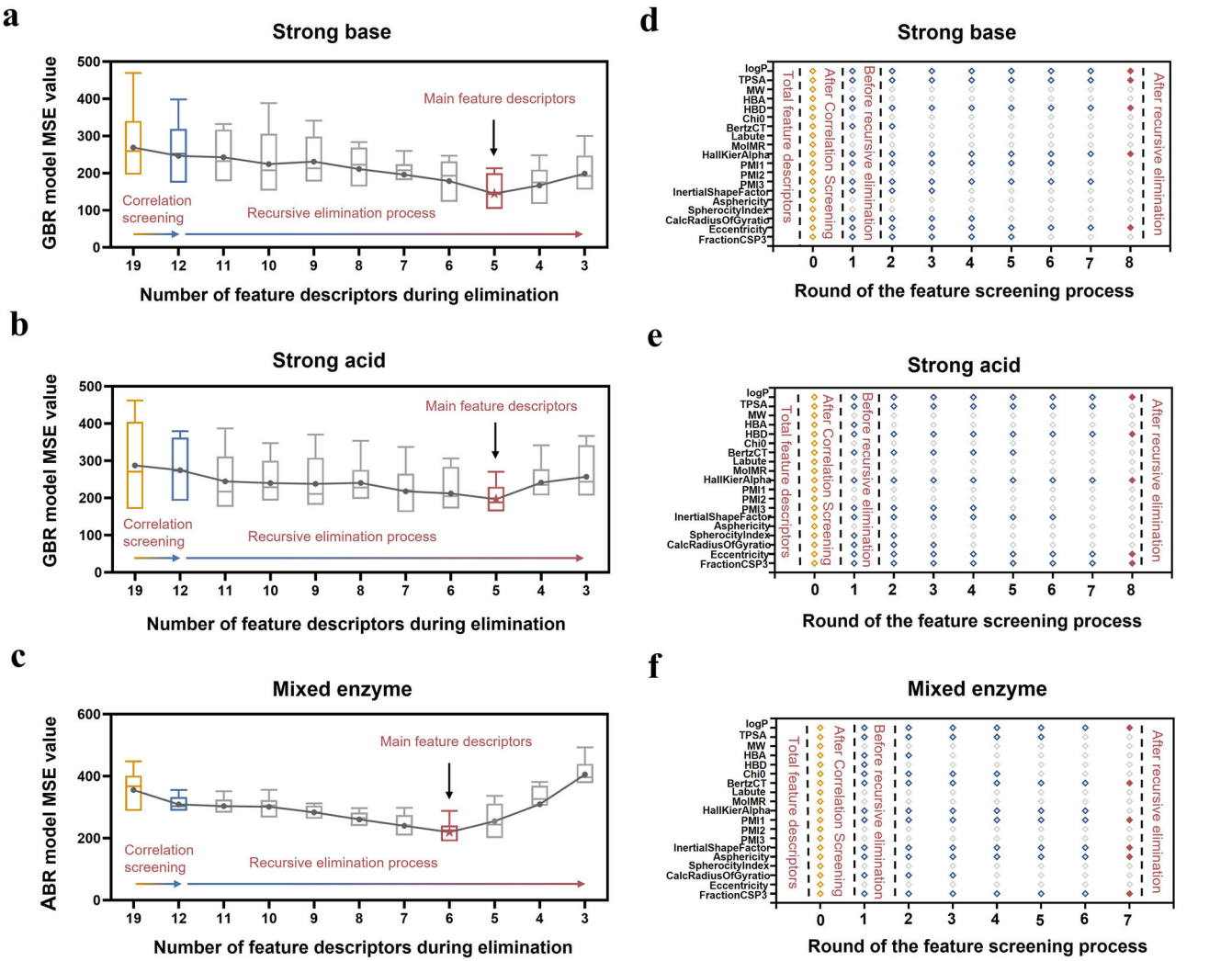

Fig. 6 | The feature screening results. Correlation screening and subsequent recursive elimination process for the input molecular feature descriptors in **a** strong base, **b** strong acid and **c** mixed enzyme dataset. The red star represented the number of the feature descriptors corresponding to the highest accurate model. Corresponding detailed process of feature screening via correlation analysis and recursive elimination in **d** strong base, **e** strong acid and **f** mixed enzyme dataset. The Y-axis was the name of the feature descriptors while the X-axis meant the round of the recursion elimination process (round 0 represented the results after the correlation screening. Yellow, blue and red rhombi represented the feature descriptors at round 0, remaining feature descriptors after each round of screening, and main feature descriptors obtained by the recursive elimination process, respectively.

stability. This set of main feature descriptors was related to all 4 categories, they were physicochemical descriptors (logP and TPSA), 2D molecular graph descriptors (HallKierAlpha and BertzCT), 3D molecular shape descriptors (Eccentricity, FractionCSP3, Asphericity and InertialShapeFactor) and hydrogen-bonding descriptors (HBD). Interestingly, the feature descriptors determining the stability of hydrogel coatings exhibited disparities in different environmental conditions. Moreover, the predicted S_{tab} values and the corresponding experimentally measured values of the three models before and after the feature screening were shown in Fig. 7. The MSE value of the models were decreased from 362 to 196 in strong base, from 299 to 145 in strong acid, and from 355 to 219 in mixed enzyme conditions, respectively. The corresponding R^2values also increased synchronously. The results demonstrated that the feature screening process using correlation screening and recursive elimination significantly improved the model prediction accuracy.

Interpretable analysis and experimental validation for machine learning models

To aid in our understanding of the hidden relationship between main molecular feature descriptors and the coating stability, a bee swarm diagram was used to summarize the SHAP values of each main feature descriptor related to the S_{tab} value. The color of each point represented the relative magnitude of the descriptor value within the entire dataset. Specifically, colors closer to deep blue and light green correspond to relatively larger and smaller values, respectively. The X-axis meant the SHAP values of each point. The absolute SHAP values quantified the magnitude of the impact of feature descriptors on hydrogel coating stability, while positive and negative values indicate enhancement or reduction of the stability, respectively. As shown in Fig. 8a–c, LogP dominated the stability performance of the polyacrylamide-based hydrogel coatings in all three environments. Generally speaking, LogP values provide an estimate of the octanol/water partition coefficient, serving as a proxy for an energetic characteristic of the molecules to describe their hydrophilicity/hydrophobicity. The SHAP values of LogP exhibited a wide and monotonic distribution, indicating that LogP was positively correlated with the stability of hydrogel coatings. Overall, hydrogel coatings with high LogP values can form a physical barrier, reducing the direct attack of environmental factors on the hydrogel network. Specifically, hydrophilic functional groups in the network, such as esters and amide bonds, are more prone to hydrolysis under base conditions.

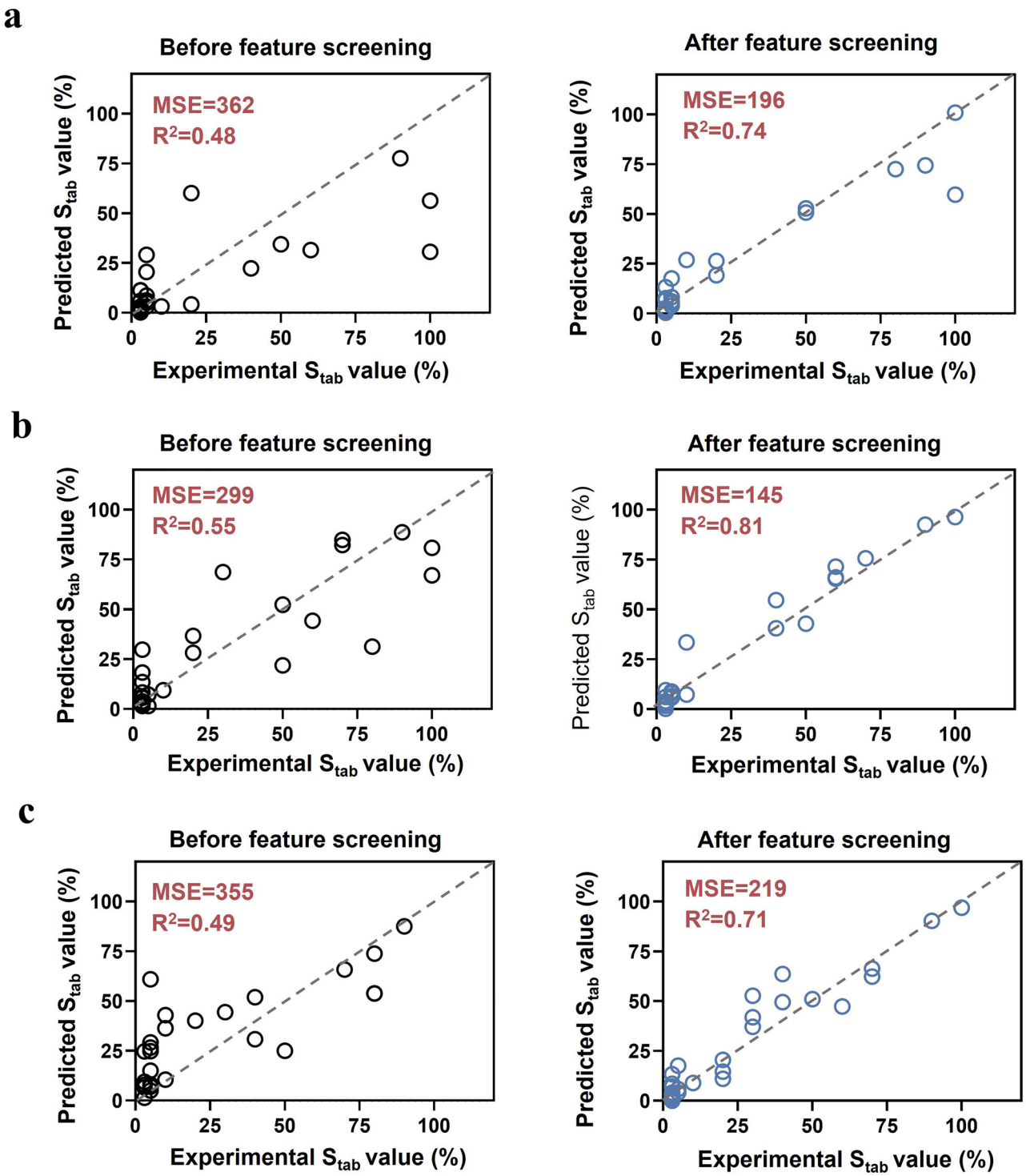

Fig. 7 | The comparison of model accuracy before and after the feature screening. The distribution of machine learning predicted values and experimental values in **a** strong base, **b** strong acid and **c** mixed enzyme dataset.

High LogP coatings reduced the exposure of these groups, thereby slowing down the hydrolysis process[41]. In acidic environments, hydrophobic molecular chains lacking protonatable sites preferentially aggregate in non-polar regions, minimizing interactions with H^+ and preventing the structural damage of the polymer network caused by protonation[42]. The hydrogel coatings with a high LogP value reduced the exposure of the catalytic site of enzymes. Therefore, LogP contributes most significantly to the stability performance of hydrogel coatings in strong base, strong acid and mixed enzyme environments.

Subsequently, the 3D molecular shape descriptors, Eccentricity and Asphericity, were found to be highly relevant to the stability of hydrogel coatings. Coatings with high Eccentricity values exhibited superior stability under base and acid conditions, while those with high Asphericity values were observed high stability in enzyme solution. Both Eccentricity and Asphericity values serve as quantitative metrics for evaluating the extent of deviation of the object between an actual geometry and its idealized theoretical form[43]. Take the calculation of Eccentricity as an example, the atom (except the hydrogen atom) and the chemical bonds in molecule graphs

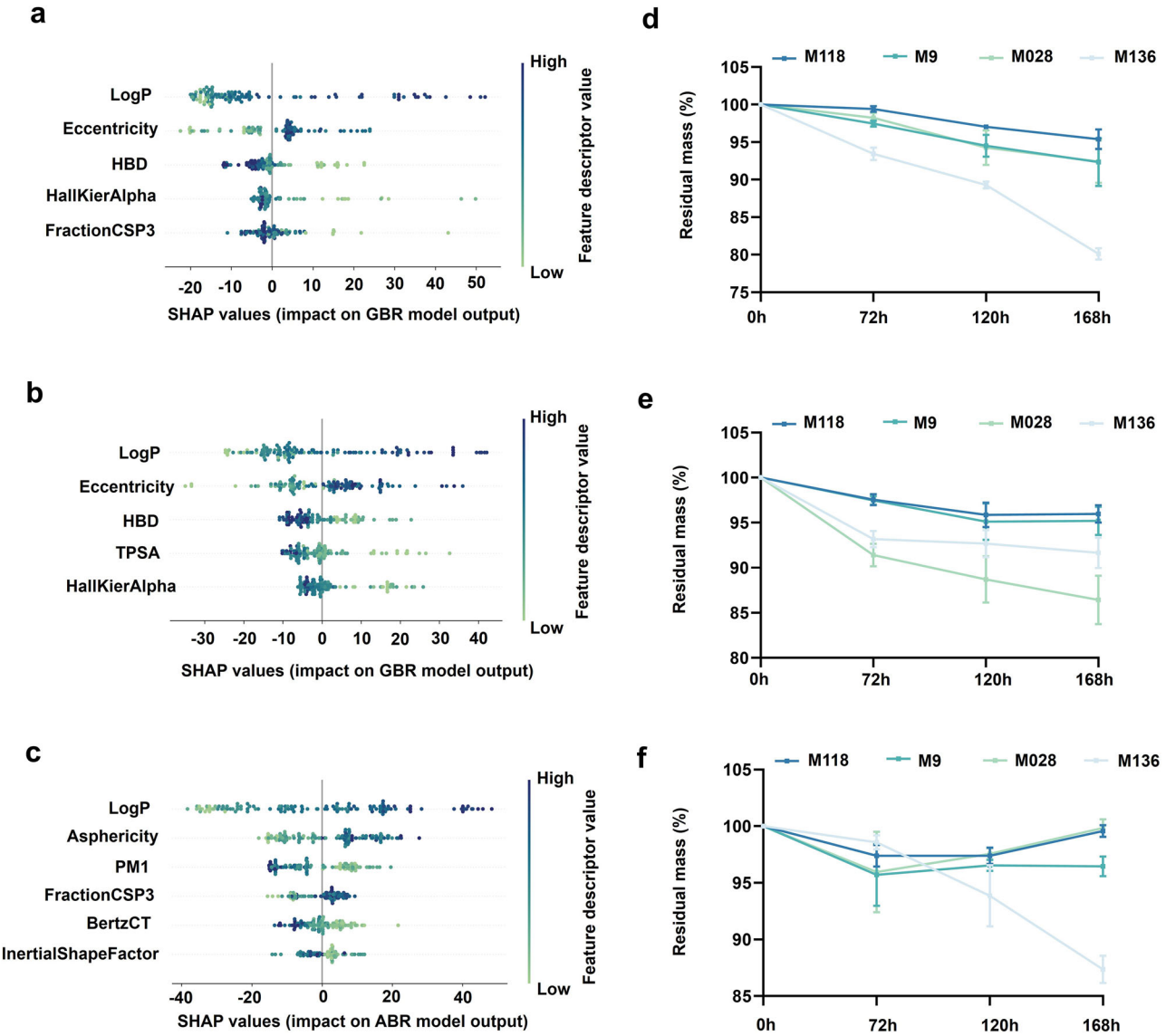

Fig. 8 | Interpretable analysis and new coating design based on the main feature descriptors. Summary of the SHAP values of main molecular feature descriptors related to the stability behavior under **a** strong base, **b** strong acid and **c** mixed enzyme environments via a bee swarm diagram. The stability of typical coatings outside the original dataset under **d** strong base, **e** strong acid and **f** mixed enzyme conditions. The three numbers in M118, M028 and M136 represented the proportions of M2, M8 and M9 in the copolymer coatings. For example, M118 represented a hydrogel coating consisting of 10% M2, 10% M8 and 80% M9.

were treated as vertices and edges, respectively. The Eccentricity value of a molecule was defined as the mean topological distance (i.e., the number of edges on the shortest path) between all pairs of vertices. Therefore, the magnitude of the eccentricity descriptor mainly reflects the extensibility or topological diameter of the molecule. Generally speaking, molecules with the following structural features tend to exhibit high eccentricity values: (i) long-chain alkanes, (ii) highly branched molecules with long arms, (iii) rigid rod-like molecules and (iv) macrocyclic molecules. The polymerization of these molecules tends to form hydrogel networks with topological chain entanglement and domains of directional alignment[44]. These polymer networks exhibited high elastic properties and have an ability to delay the penetration of corrosive media, thus exhibiting a strong impact on the stability of hydrogel coatings[45]. This finding agrees with the other work, which emphasizes the importance of polymer chain entanglement and asymmetrical network topology in determining the solvent resistance and increasing mechanical properties of hydrogels via NeTHE model[46].

Moreover, HBD was also discovered to contribute a lot to coating stability. HBD is used to quantify the number of atoms or groups in a molecule that can act as hydrogen bond donors. In this work, HBD was identified to have a negative correlation with the stability of hydrogel coatings, i.e., the coating had fewer hydrogen bond donors in the polymer network exhibited better stability in base and acid environments. In general, high hydrogen bond density contributes to improved mechanical properties and stability of hydrogel coatings[47]. However, in base environments, the presence of abundant H^+ ions led to the protonation of hydrogen bond donor sites, resulting in the dissociation of polymer network. Similarly, the OH^- of base environment could destroy the hydrogen bond donors via deprotonation effect, leading to an increase in the swelling rate and a decrease in the mechanical properties of the hydrogel coating. It is worth noting that, HBD molecular descriptor does not exhibit a dominant effect on the stability of the hydrogel coating after immersing in the mixed enzyme solution. This result was due to that the mixed enzyme solution exhibited a neutral pH, which would not cause the protonation or deprotonation of the HBD hydrogen bond donor groups. The degradation mechanism of the enzyme solution to the hydrogel coating is considered to be the catalysis of specific substrates and is irrelevant to HBD[48].

To verify the rationality of the feature identification results, the machine learning models built in this work were used to predict the

stability of a large number of ternary hydrogels prepared from the combination of monomers M1 to M9. Similarly, the feature descriptors for the ternary hydrogel coatings were obtained by calculating the weighted average of monomer descriptor values according to the specific coating composition. According to the prediction results, we designed three new hydrogel coatings outside the original dataset and two of them were ternary. These coatings were composed of M2, M8, and M9 in different proportions, and were predicted with relatively high Stab value in all three environments. According to the specific compositions, these coatings were named M118, M028 and M136, respectively. The details of these coating compositions were reported in Table S2. For instance, M118 denotes a hydrogel coating composed of 10% M2, 10% M8, and 80% M9 by molar ratios. Fig. 8d–f showed the stability of M118, M028, M136 and M9 (the typical single-component coating in the original dataset) hydrogel coating under strong base, strong acid and mixed enzyme conditions. Among these, M118 and M028 samples exhibited superior stability to M9 during 168 h. Especially, the weight loss of M118 under all three conditions was less than 5%. Benefiting from the elaborate screening of main features, the advanced strategy successfully designed a ternary hydrogel coating with high stability in harsh environments by utilizing the labeled data obtained from single and binary coatings. The filtered list of feature descriptor candidates that significantly influenced the stability of hydrogel coatings can provide effective guidance for the design of long-term usable coatings. More interestingly, researchers have developed an advanced multi-objective property molecular optimization framework in a recent study. By leveraging the contribution of molecular feature descriptors to the target properties with scarce labeled data, they achieved the multi-objective optimization of molecular performance through structural modifications of molecules that have been optimized for a single target property with sufficiently labeled data[49]. Although the insufficient stability of hydrogel coating would severely hinder their service performance, current data and feature analyses regarding coating stability remain scarce. The revealed contribution of molecular features to hydrogel coating stability in this work provided a solid foundation for the knowledge transfer from single-attribute datasets to complex multi-objective optimization, thus playing a crucial role in the rational design of various functional hydrogel coatings with satisfying stability.

Discussion

In this work, a miniaturized high-throughput hydrogel coating preparation and measurement strategy was developed based on automated coating microarray technology. This strategy evaluated the stability of a series of hydrogel coatings with various components and formulations in a convenient and rapid manner. Benefiting from the creation of a library consisting of 117 unique hydrogel coatings, a feature screening and interpretable machine learning method was used to identify the main molecular features giving rise to the stability of all hydrogel coatings we tested. Interpretable machine learning analysis demonstrated that the relevant mechanisms underlying the stability of polyacrylamide-based hydrogel coatings in harsh environments arise from hydrophobicity and asymmetric 3D structure in the polymer network. We also demonstrated that the number of hydrogen bond donors in the polymer network exhibited a negative correlation to the coating stability in base and acid environments, but was irrelevant to the coating stability in enzyme solution. The results can be explained by the fact that the degradation mechanism of the enzyme does not involve the protonation or deprotonation of hydrogen bond donor groups in the network. Based on the main feature descriptors, a new ternary hydrogel coating with a well-tailored formulation was prepared and exhibited superior stability under harsh conditions. The discovery and explanation of the main feature descriptors that significantly determine the stability of hydrogel coatings hold great promise for the rational design of functional hydrogel coatings for longer-term use.

Methods

Materials

The acrylamide derivative monomers used to create the hydrogel-based coating library covered diverse structures and functionalities, including acrylamide (M1), diethylacrylamide (M2), hydroxymethylacrylamide (M3), hydroxyethylacrylamide (M4), acryloylmorpholine (M5), (acrylamidopropyl)trimethyl-ammonium (M6), 2-acrylamido-2-methyl-propane sulfonic acid (M7), dimethylacrylamide (M8), N-isopropylacrylamide (M9). These monomers, and oxygen scavenger glucose oxidase and D-(+)-glucose were purchased from Sigma-Aldrich. The crosslinker bis-acrylamide, photoinitiator 2-hydroxy-4'-(2-hydroxyethoxy)-2-methylpropiophenone and fluorescein (rhodamine B and Congo red) were purchased from Aladdin Industrial Corporation. Lysozyme (100,000 U/g) and lipase (40,000 U/mg) were purchased from Macklin Biochemical Technology Co., Ltd. The monomers were purified by Alumina B to remove the polymerization inhibitor prior to use. Other materials were used as received without further purification. The 316 L stainless steels ($80 \times 60 \times 1$ mm^3) were used to be coated as an example substrate because they have decent corrosion resistance and are widely used for medical devices. Before use, 316 L substrates were abraded by grit abrasives (400#, 800#, and 1500#) and subsequently cleaned in ethanol under ultrasonication.

Automated hydrogel coating microarrays preparation

Using a non-contact droplet microarray printer (Nano-Plotter™ NP2.1, GeSiM, Germany), the hydrogel coatings were automatically prepared via photoinduced free radical polymerization on 316 L substrates. The sequences and processes to be conducted by this printer were pre-programmed, indicating information on sample types, reagent volumes, and pipetting positions. This printer utilizes non-contact picolitre liquid-dispensing technology, featuring piezoelectric pipetting tips for precise control over droplet formation. Real-time image feedback allows accurate monitoring of the dispensing process, ensuring the repeatability of the experiment. As for monomer solution, the printer incorporates a heating module (up to 120 °C) that facilitates the dispensing of high-viscosity liquids. Compared with the traditional single synthesis experiments in separate vials, this high-throughput method offers a significant reduction in dose requirements and time-consuming[18]. Before the coating preparation, 1 g of monomers was dissolved in 1 mL of Milli-Q water to prepare the solution. The crosslinker and photoinitiator were dissolved to prepare the solution with a concentration range of 25 mg mL^{-1} to 50 mg mL^{-1}. We set the volume of a single droplet burst to 400 pL and adjusted the number of droplets for each component in the software as needed prior to the printing process. Solution dosages were optimized and validated before and after dispensing to enable precise picolitre-level printing. Note that the presence of oxygen could dramatically decrease the efficiency of photoinitiated free radical polymerization. Thus, 40 μM of glucose oxidase and 0.1 M D-(+)-glucose solution was used for every experiment as an oxygen scavenger system[25].

A typical process to print and synthesize the hydrogel spots includes printing of 40 droplets of acrylamide (M1), overprinting with 40 droplets of diethylacrylamide (M2), overprinting 320 droplets of crosslinker bis-acrylamide and photoinitiator solution supplemented with glucose oxidase and glucose. Subsequently, the droplet microarray was irradiated (30 s, 60 mW cm^{-2}) for photoinitiated polymerization. The humidity was maintained at 80% RH during the printing process to avoid droplet evaporation. Following the above steps, a hydrogel spot with a monomer ratio of 1:1 (M1: M2), a monomer content of 20%, and a crosslinker content of 10% could be obtained. In this work, hydrogel microarrays consisting of single and binary combinations of various acrylamide-based monomers were prepared. The microarrays consisted of hydrogel spots with multiple monomer ratios, monomer contents, and crosslinker contents.

For fluorescence measurements, the fluorescein and rhodamine B were introduced into different monomer solutions respectively before the printing process. Then, the hydrogel spot was printed and synthesized in the way described above. The fluorescein and rhodamine B could be excited with green and red fluorescence under fluorescence microscopy, respectively.

Miniaturized high-throughput evaluation for the stability of hydrogel coatings

The stability of the polyacrylamide-based hydrogel coatings was evaluated by immersing these microarrays in the solutions of 6 M NaOH, 10 wt.% H_2SO_4 and 1 mg mL^{-1} enzyme (lysozyme and lipase), respectively. These expedited degradation conditions were chosen to match the biodegradation environments[26]. During the experiment, the microarrays were placed in a closed petri-dish containing 30 mL solution and allowed to stand at 30 °C for 72 h. After immersing, the microarrays were washed three times with ethanol and dried with argon gas before evaluation. Subsequently, the digital images of the hydrogel microarrays were taken. The retained area of the hydrogel spots after the immersion was quantified to evaluate the stability of each coating using software ImageJ. Miniaturized evaluation steps were as follows: (i) The original digital images of hydrogel microarrays were converted to single-channel 8-bit pixels; ii) Setting threshold to delineate the retained area of hydrogel spot images while removing background; (iii) Automatically calculating the retained area of the hydrogel spots via 'Analyze Particles' instructions. The stability (S_{tab}) value of each hydrogel coating could be calculated as following Eq. (1).

$$S_{tab} = \frac{\mathrm{Area}_{exp}}{\mathrm{Area}_{con}} * 100\% \quad (1)$$

where Area_{exp} and Area_{con} represent the retained area value of experimental samples and intact samples, respectively.

Machine learning data analysis

Machine learning models were implemented in *scikit-learn* 0.20.2 to analyze the high-throughput experimental results of polyacrylamide-based hydrogel coatings. Five regression algorithms were employed to construct predictive models, including support vector regression (SVR), adaptive boosting regression (ABR), gradient boosting regression (GBR), artificial neural network (ANN) and gaussian process regression (GPR). Each approach offers a unique pattern to recognize the hidden relationships in large datasets. The introduction of these machine learning models was presented in Note 1 (*Supporting Information*). The grid search was used for hyperparameter optimization of each model. The dataset was randomly partitioned into 80% training and 20% testing subsets. 100 models of these five algorithms were obtained through 100 different samplings. The mean values of mean-squared error (MSE) and coefficient of determination (R^2) of these 100 interactions were taken as the metric to reflect the prediction capability of the model, using Eqs. (2) and (3), respectively.

$$\mathrm{MSE} = \frac{1}{n}\sum_{k=1}^{n}(y_k - \tilde{y}_k) \quad (2)$$

$$R^2 = 1 - \frac{\sum_{k=1}^{n}(y_k - \tilde{y}_k)^2}{\sum_{k=1}^{n}(y_k - \bar{y})^2} \quad (3)$$

where n represents sample count, y_k and $\tilde{y}_k$ denotes experimental values and predicted values. A lower MSE value and larger R^2 value indicated a higher prediction accuracy of the machine learning model.

A two-step feature screening method based on the best-performing model was applied for machine learning dimensionality reduction. First, the Pearson correlation coefficient r was used to identify the correlation among features as following Eq. (4).

$$r = \frac{\sum\left[(x_i - x_m)\times(y_i - y_m)\right]}{\sqrt{\sum(x_i - x_m)^2}\sqrt{\sum(y_i - y_m)^2}} \quad (4)$$

where x_i and y_i represents the values of two input features in the i-th hydrogel coating, x_m and y_m represents the average values of these two features in all hydrogel coatings. The two features with value $|r| > 0.95$ exhibited strong linear correlation, indicating the same or similar influences for hydrogel coating properties. In such cases, the features exhibiting higher prediction error were removed because they were redundant for machine learning prediction. Second, recursive elimination was used to further screen the important features. For each iteration, one of the n features was temporarily excluded while the remaining $n - 1$ features formed the input vector for model training. The features corresponding to the smallest model error were removed and the remaining $n - 1$ features proceeded to the next iteration. Recursive elimination was performed until the minimum model error demonstrated a transition from a reduction to an increment trend, signaling diminishing returns for further feature reduction.

Model interpretability was achieved via SHapley Additive exPlanations (SHAP) analysis. SHAP regards each input feature as a contributor to model output, applying cooperative game theory principles to quantify feature contribution. Each input feature received a SHAP value representing its marginal contribution size and the contribution direction (positive or negative). This methodology enabled systematic identification of the main features that determined the stability of polyacrylamide-based hydrogel coatings under harsh conditions.

Experimental verification

The four hydrogel coating formulations exhibiting the highest stability predicted by the machine learning strategy were selected for scale-up verification experiments. 316 L stainless steel ($10 \times 10 \times 3$ mm^3) was dipped into the hydrogel prepolymer solution and polymerized for a short time and removed immediately. Then, an additional 30 s curing was taken to ensure the complete polymerization. Hydrogel coatings were immersed in the same solutions (6 M NaOH, 10 wt.% H_2SO_4 and 1 mg mL^{-1} enzyme) at 30 °C for up to 72 h. At each time interval, hydrogel coatings were removed from the solution and placed into deionized water overnight. Samples were freeze-dried and the weights were recorded to determine their stability.

Data availability

The main data supporting the findings of this work are available within the Article and its Supplementary Information.

Code availability

The datasets and code for this work is not publicly available but may be made available to qualified researchers on reasonable request from the corresponding author.

Received: 24 July 2025; Accepted: 3 November 2025;
Published online: 04 December 2025

References

1. Taylor, D. & Panhuis, M. Self-healing hydrogels. *Adv. Mater.* **28**, 9060–9093 (2016).
2. Gao, L. et al. Multi-responsive, bidirectional large deformation Bending actuators based borax cross-linked polyvinyl alcohol derivative hydrogel. *RSC Adv.* **162**, 40005 (2017).
3. Xie, W. et al. Injectable and self-healing thermosensitive magnetic hydrogel for asynchronous control release of doxorubicin and docetaxel to treat triple-negative breast cancer. *ACS Appl. Mater. Interfaces* **9**, 33660–33673 (2017).
4. Xu, R. et al. A universal strategy for growing a tenacious hydrogel coating from asticky initiation layer. *Adv. Mater.* **34**, 2108889 (2012).
5. Magin, C., Cooper, S. & Brennan, A. Non-toxic antifouling strategies. *Mater. Today* **13**, 36–44 (2010).
6. Hua, Y. et al. Ultrafast, tough, and adhesive hydrogel based on hybrid photocrosslinking for articular cartilage repair in water-filled arthroscopy. *Sci. Adv.* **7**, eabg0628 (2021).
7. Liu, J., Qu, S., Suo, Z. & Yang, W. Functional hydrogel coatings. *Natl. Sci. Rev.* **8**, nwaa254 (2021).
8. Li, S. et al. Anti-swelling, and antibacterial hydrogels for tooth-extraction wound healing. *Adv. Healthc. Mater.* **13**, 2400089 (2024).

9. Ren, Z. et al. Strong and anti-swelling nanofibrous hydrogel composites inspired by biological tissue for amphibious motion sensors. *Mater. Horiz.* **11**, 5600–5613 (2024).
10. Mredha, M. et al. Hydrogels with superior mechanical properties from the synergistic effect in hydrophobic–hydrophilic copolymers. *Chem. Eng. J.* **362**, 325–338 (2019).
11. Guan, X. et al. Preparation of environmental resistance and anti-swelling hydrogel through solvent displacement for monitoring human health and movement in amphibious environment. *Chem. Eng. J.* **505**, 159838 (2025).
12. Haraguchi, K., Xu, Y. & Li, G. Molecular characteristics of poly(N-isopropylacrylamide) separated from nanocomposite gels by removal of clay from the polymer/clay network. *Macromol. Rapid Commun.* **31**, 718–723 (2010).
13. Dai, S. et al. Tough hydrogel–elastomer hybrids hydrophobically regulated by an MXene for motion monitoring in harsh environments. *J. Mater. Chem. C.* **11**, 2688–2694 (2023).
14. Li, M. et al. Recent advances in hydrogel-based flexible strain sensors for harsh environment applications. *Chem. Sci.* **15**, 17799 (2024).
15. Butler, K. et al. Machine learning for molecular and materials science. *Nature* **559**, 547–555 (2018).
16. Xu, T. Accelerating the prediction and discovery of peptide hydrogels with human-in-the-loop. *Nat. Commun.* **14**, 3880 (2023).
17. Xu, S. et al. Integrating machine learning for the optimization of polyacrylamide/alginate hydrogel. *Regen. Biomater.* **11**, rbae109 (2024).
18. Yang, J. et al. High-throughput screening of zwitterion-based coatings towards improved mechanical stability and drug-loading capacity. *npj Mater. Degrad.* **7**, 51 (2023).
19. Sánchez-Morán, H., Kaar, J. & Schwartz, D. Combinatorial high-throughput screening of complex polymeric enzyme immobilization supports. *J. Am. Chem. Soc.* **146**, 9112–9123 (2024).
20. Yang, J. et al. Synergistic D-amino acids based antimicrobial cocktails formulated via high-throughput screening and machine learning. *Adv. Sci.* **11**, 2307173 (2024).
21. Zhong, M. et al. Accelerated discovery of CO_2 electrocatalysts using active machine learning. *Nature* **581**, 178–183 (2020).
22. Sun, S. et al. Accelerated development of perovskite-inspired materials via high-throughput synthesis and machine-learning diagnosis. *Joule* **3**, 1437–1451 (2019).
23. Dave, A. et al. Autonomous optimization of non-aqueous Li-ion battery electrolytes via robotic experimentation and machine learnin coupling. *Nat. Commun.* **13**, 5454 (2022).
24. Seifermann, M. et al. High-throughput synthesis and machine learning assisted design of photodegradable hydrogels. *Small Methods* **7**, 2300553 (2023).
25. Rosenfeld, A. et al. Miniaturized high-throughput synthesis and screening of responsive hydrogels using nanoliter compartments. *Mater. Today Bio* **6**, 100053 (2020).
26. Yan, P. et al. Water dynamics in polyacrylamide hydrogels. *J. Am. Chem. Soc.* **140**, 9466–9477 (2018).
27. Jiao, Z. et al. Drug-free contact lens based on quaternized chitosan and tannic acid for bacterial keratitis therapy and corneal repair. *Carbohydr. Polym.* **286**, 119314 (2022).
28. Sun, J. et al. Highly stretchable and tough hydrogels. *Nature* **489**, 133–136 (2021).
29. Chan, D. et al. Combinatorial polyacrylamide hydrogels for preventing biofouling on implantable biosensors. *Adv. Mater.* **34**, 2109764 (2022).
30. Chou, Y. et al. Ultra-low fouling and high antibody loading zwitterionic hydrogel coatings for sensing and detection in complex media. *Acta Biomater.* **40**, 31–37 (2016).
31. Yu, Y. et al. Slippery, and anticoagulant double-network hydrogel coating. *ACS Appl. Polym. Mater.* **4**, 5941–5951 (2022).
32. Li, M. et al. Hydrogel coatings of implants for pathological bone repair. *Adv. Healthc. Mater.* **13**, 2401296 (2024).
33. Yao, M. et al. Microgel reinforced zwitterionic hydrogel coating for blood-contacting biomedical devices. *Nat. Commun.* **13**, 5339 (2022).
34. Bentéjac, C., Csörgo, A. & Martínez-Muñoz, G. A comparative analysis of gradient boosting algorithms. *Artif. Intell. Rev.* **54**, 1937–1967 (2021).
35. Danielsen, S. et al. Molecular characterization of polymer networks. *Chem. Rev.* **121**, 5042–5092 (2021).
36. Xiao, Z. et al. Adhesion mechanism and application progress of hydrogels. *Eur. Polym. J.* **173**, 111277 (2022).
37. Yang, J. et al. Hydrogel adhesion: A supramolecular synergy of chemistry. *Adv. Funct. Mater.* **30**, 1901693 (2020).
38. Yang, J. et al. Combinatorial discovery and investigation of the synergism of green amino acid corrosion inhibitors: integrating high-throughput experiments and interpretable machine learning approach. *Corros. Sci.* **245**, 112675 (2025).
39. Liu, S. et al. Towards understanding and prediction of corrosion degradation of organic coatings under tropical marine atmospheric environment via a data-driven approach. *Int. J. Miner. Metall. Mater.* **32**, 1151–1161 (2025).
40. Zhang, H. et al. Empowering the Sustainable Development of High-End Alloys via Interpretive Machine Learning. *Adv. Mater.* **36**, 2404478 (2024).
41. Dong, L. et al. Hydrogel antifouling coating with highly adhesive ability via lipophilic monomer. *Macromol. Mater. Eng.* **307**, 2100812 (2022).
42. Jiang, L. et al. Real-time monitoring of hydrophobic aggregation reveals a critical role of cooperativity in hydrophobic effect. *Nat. Commun.* **8**, 15639 (2017).
43. Todeschini, R. & Consonni, V. Handbook of chemoinformatics: from data to knowledge (ed. Gasteiger, J.) 1004–1033 (Wiley-VCH, 2003).
44. Kim, S., Schroeder, M. & Jackson, N. Functional monomer design for synthetically accessible polymers. *Chem. Sci.* **16**, 4755–4767 (2025).
45. Cui, H. et al. Hydrophobic hydrogels as internal curing agent for concrete: the double benefit of super high water content and excellent anti-ion permeability. *Compos. Commun.* **33**, 101236 (2022).
46. You, H. et al. A model with contact maps at both polymer chain and network scales for tough hydrogels with chain entanglement, hidden length and unconventional network topology. *Int. J. Mech. Sci.* **262**, 108713 (2024).
47. Han, Z. et al. A versatile hydrogel network-repairing strategy achieved by the covalent-like hydrogen bond interaction. *Sci. Adv.* **8**, eabl5066 (2022).
48. Feng, R. et al. Mechanisms of efficient polyacrylamide degradation: from multi-omics analysis to structural characterization of two amidohydrolases. *Int. J. Biol. Macromol.* **281**, 136329 (2024).
49. Wu, Z. et al. Leveraging language model for advanced multiproperty molecular optimization via prompt engineering. *Nat. Mach. Intell.* **6**, 1359–1369 (2024).

Acknowledgements

This work is financially supported by the Advanced Materials-National Science and Technology Major Project (2024ZD0607500), Postdoctoral Fellowship Program of CPSF under Grant Number GZC20240101, Guangdong Basic and Applied Basic Research Foundation (2021B1515130009).

Author contributions

J.Y.: Writing – original draft, Investigation, Conceptualization, Methodology. Y.R.: Investigation. Y.J.: Investigation, Validation. A.K.: Investigation. M.Z.: Investigation. L.M.: Supervision, Validation. D.Z.: Supervision, Conceptualization, Writing – review & editing.

Competing interests

As the Associate Editor and Editorial Board Member, L.M. and D.Z. were not involved in the peer-review or decision-making process for this manuscript, which was managed entirely by independent editors. The authors affirm that

their editorial roles have not influenced the content or conclusions of this work. The other authors declare no competing interests.

Additional information

Supplementary information The online version contains supplementary material available at https://doi.org/10.1038/s41529-025-00706-3.

Correspondence and requests for materials should be addressed to Lingwei Ma or Dawei Zhang.